Desalination and Water Treatment
www.deswater.com

doi:10.5004/dwt.2018.22236

111 (2018) 22–31
April

High desalination performance of reverse osmosis membrane incorporating single-walled carbon nanotubes with tip and inner modification

Jianhua Wang[a,†], Dengfeng Yang[a,†], Jinsheng Shi[a], Qing Li[b], Qingzhi Liu[a,*]

[a]*College of Chemistry and Pharmaceutical Science, Qingdao Agriculture University, No. 700 Changcheng Road, Qingdao City 266109, China, Tel. +86-15689130072, email: 1140190376@qq.com (J. Wang), Tel. +86-13370829189, email: dfyang@qau.edu.cn (D. Yang), Tel. +86-15275201860, email: jsshiqn@163.com(J. Shi), Tel. +86-0532-86080895, +86-18669861398, email: liuqz2001@163.com (Q. Liu)*

[b]*College of chemistry, Beijing Normal University, Beijing 100875, China, Tel. +86-17801161386, email: liqing8282@163.com (Q. Li)*

Received 11 October 2017; Accepted 24 March 2018

ABSTRACT

To enhance the desalination of reverse osmosis membranes, thin film nano composite reverse osmosis membranes were prepared by inter-facial polymerization that trimesoyl chloride (TMC) solution in n-hexane blended in aqueous solutions of m-phenylenediamine (MPD) containing modified single-walled carbon nano tubes (SWCNTs) (0.93 nm diameter). The functionalized SWCNTs were obtained by chemical process and analyzed by TGA, XPS, and HRTEM, etc. The experimental results showed that the expected functional groups were successfully grafted on the tip and inner wall of the single-walled carbon nano tubes. The surface characteristics of membranes were studied in SEM images, salt rejection, water flux tests and surface contact angle analysis. Membrane performance test showed that the water flux and salt rejection were significantly increased for modified SWCNT-polyamide thin film nano composite membranes (especially those containing hydrophilic groups such as carboxyl groups and amino groups) compared with the bare polyamide membrane.

Keywords: Single-walled carbon nano tubes; Inner/surface modification; SWCNTs-polyamide nano composite membranes; Desalination

1. Introduction

Carbon nano tubes (CNTs) have been studied since they were discovered by Iijima [1] in 1991. A great many but unique properties of CNTs including extraordinary chemical, physical, and mechanical properties have aroused a worldwide interests [2–6]. Despite of the excellent performance of CNTs, there still existed some problems to be solved such as easily to reunite, bad dispersion in organic solvents and weak interaction between the CNTs and the polymer matrix, etc. which restrained their application.

To enhance the hydrophilicity and the dispersity of carbon nano tubes as well as the intensified adhesion to the polymer, different strategies have been reported, such as enhancing adhesion strength between carbon nano tubes and substrate interface by covalent bond [7,8], functionalization by chemical agents and attaching polar groups to CNT sidewalls [9–13] or inner walls [14–16], etc. These experimental results showed that the oxidation of CNTs could not only remove the residual impurities in process of preparation, but introduce oxygen-containing functional group and improve the dispersion of CNTs in polar solvent. More importantly, it allowed the structure of CNTs for further modification.

Reverse osmosis (RO) membranes are widely used in commercial RO systems due to the low cost, high energy efficiency and sample operation. However, the disadvantages of low water flux, low salt rejection, low antifouling and poor dispersity delay its space. So, some researchers made efforts to modify the reverse osmosis membranes. For example, Farahbakhsh et al. [17–19] and Rahimpour et al. [20] prepared polyamide reverse osmosis membrane with functionalized

*Corresponding author.

†This two authors contributed equally in this article.

CNTs and investigated the effects of polyamide reverse osmosis membrane containing raw and oxidized carbon nano tubes on the desalination, water flux, and fouling resistance. Other researchers [21–23] synthesized the polyamide/MWNTs reverse osmosis membrane with high membrane performance and observed the effects of the amount of carbon nano tubes on water flux and desalination. Experimental results showed that the flux and salt rejection of membranes increased by addition to proper concentrations of modified MWCNTs, and the membranes fouling resistance was improved by reducing surface roughness and increasing hydrophilicity of the membrane surface.

Our researching group has done a series of simulations on water flux and salt rejection of modified single-walled and multi-walled carbon nano tubes [24,25]. The results showed that when certain number and type of functional group (–COOH, $–CONH_2$ and $–NH_2$) were added to the interior and/or on the tip of single-walled (10,10) (1.356 nm) or (13,13) (1.763 nm), 100% salt rejection could be obtained with high water flux (13 times of the traditional reverse osmosis membrane). In view of that, a series of tip and inner wall modification of SWCNTs (with 0.93 nm inner diameter) were directly conducted in this article and then thin film nano composite reverse osmosis membranes by incorporating functionalized single-walled carbon nano tubes (SWCNTs) were prepared by interfacial polymerization.

2. Experiments

2.1. Materials and solvents

Single-walled carbon nano tubes (SWCNTs) (purity > 95%, diameter 0.93 nm, length 5-30 μm, Ash < 0.5wt%, SSA > 450 m^2/g, EC > 100 s/cm), sulfuric acid (95–98%), nitric acid (65–68%), pyridine (Py), dimethylformamide (DMF), thionyl chloride ($SOCl_2$), ammonium carbonate ($(NH_4)_2CO_3$), tetrahydrofuran (THF), methanol, sodium, bromine, PTFE membrane (diameter 50 mm, pore size 0.22 μm). Polysulfone (PSF) membranes, m-phenylenediamine (MPD, 99%), trimesoyl chloride (TMC, 98%), n-hexane (97%).

2.2. Preparation of functionalized SWCNTs

Since SWCNTs are generally bundled, pristine SWCNTs were immersed in 60 ml of concentrated H_2SO_4/HNO_3 (3:1, v/v) solution at 60°C and treated by stirring reflux for 6 h (Oxidized SWCNTs were prepared by an optimized reaction condition, the maximum graft rate was confirmed by TGA). The resulting solution was diluted by deionized water and vacuum-filtered in PTFE membrane until the PH of the filtrate turned to be neutral. The obtained SWCNT-COOH was dried under vacuum drying oven at 60°C for 12 h.

Three hundred and fifty mg SWCNT-COOH was stirred in an excess mixture solution of DMF and $SOCl_2$ (1:5) at 85°C for 30 h. The main purpose of this process is to convert the carboxylic acids into acyl chlorides. An excess of $SOCl_2$ was removed by reduced pressure distillation. The product (SWCNT-COCl) was washed by THF and vacuum-filtered in PTFE membrane and then dried under vacuum at 60°C for 12 h.

Two hundred mg of SWCNT-COCl was added into 15000 mg $(NH_4)_2CO_3$ suspension which was dispersed in 50 ml DMF, then 50 ml pyridine was added slowly into the reactor under continuous stirring at room temperature. Subsequently, the solution was treated by stirring reflux at 70°C for 46 h. The product was obtained by PTFE membrane and washed with water and ethanol individually. Finally, the product ($SWCNT-CONH_2$) was dried in vacuum drying oven at 60°C for 12 h.

To get amino SWCNTs, about 1300 mg Na was immersed in 100 ml methanol, and the resulting solution was mixed with 2 ml bromine and 100 mg $SWCNT-CONH_2$. The mixed solution was stirred at 70°C for 24 h and then 1 ml Br_2 were dropped in followed by another 24 h continuous stirring. The collected black solid was filtered and then washed with saturated sodium carbonate, water and ethanol separately. The solid product ($SWCNT-NH_2$) was dried at 60°C for 12 h.

2.3. Characterization of SWCNTs

The modified SWCNTs were confirmed with X-ray photo electron spectroscopy analysis (XPS, Thermol scientific, Escalab 250Xi). The graft ratio was characterized by Thermo-gravimetric analyzer (STA 449 F3, NETZSCH. A sample was heat-treated at a linear heating rate of 10°C/min up to 800°C in a mixture of nitrogen and oxygen as protective gas). The morphology and the wall thickness of the samples were observed with High resolution Transmission Electron Microscope (HRTEM, JEM2100F).

2.4. Fabrication and characterization of polyamide membrane with SWCNTs and without SWCNTs

The 0.02 g of the various types of SWCNTs were dispersed in 100 mL of 2.0 wt% MPD aqueous solution to prepare the 0.02wt% CNT-dispersed solution, respectively. A PSF ultra filtration membrane was taped to a glass plate mold and fixed with four clamps. Then the film was washed for several times with ultra pure water to remove the impurities and blow off moisture and bubbles on the surface with N_2. To start the interfacial polymerization, 100 mL of 2.0 wt% MPD aqueous solution including 0 wt% SWCNTs and a various types of the 0.02 wt% SWCNTs (P-SWCNTs, SWCNT-COOH, $SWCNT-CONH_2$, $SWCNT-NH_2$) were respectively poured onto the top surface of the PSF substrate in the glass plate mold, which was horizontally held for 5 min to ensure the penetration of MPD solution into the pores of the substrate. After that, the MPD solution was poured out, andthe residual solution on the film surface was removed with N_2. One hundred mL of 0.2 wt% TMC solution in n-hexane was continuously poured onto the substrate surface for up to 30 s. Then, the membrane was taken out and placed in the 80°C oven for 10 min. The polyamide membranes with the various types of SWCNTs (PA-0, PA-SWCNTs, PA-SWCNT-COOH, PA-$SWCNT-CONH_2$, PA-$SWCNT-NH_2$) were abbreviated as PA, PA–CNT1, PA–CNT2, PA–CNT3, PA–CNT4 membrane, respectively.

The morphology of membrane surface was observed with scanning electron microscopy (SEM) (S-4800; JEOL 7500F, Japan). The hydrophilicity of membrane surface was characterized by contact angle goniometer (DSA100, Germany). The contact angles of samples were measured by 1

μl water at room temperature, and the average of at least six measurements at different locations of the sample were observed. Water flux and salt rejection were evaluated by membrane performance evaluation instrument (GY70-6, China, the pressure was maintained at about 2.0 MPa) and conductivity meter (DDS-307, China).

2.5. Membrane filtration test

Filtration experiments were conducted by lab-scale cross-flow membrane test unit with the effective filtration areas being $2 \times 2 \times \pi$ cm^2 and $3 \times 3 \times \pi$ cm^2 with the 0.3 cm of channel height, respectively. The pressure was maintained at about 2.0 MPa and the feed solution was 2000 mg/L NaCl solution (pH = 8) whose conductivity was about 3.0 m S/cm in this study. The temperature was controlled at 25°C. These membrane filtration conditions have been generally used in BWRO membrane systems by others [26,27]. Cross flow velocity at the membrane surface was 1 L min^{-1} in the filtration system. Water flux was measured by weighing the permeate solution after the membranes were compressed for 2 h at 2.0 MPa and permeated water was collected for 1 min. Membrane flux, J, was calculated using Eq. (1):

$$J = \frac{\Delta V}{A \times \Delta t} \tag{1}$$

where ΔV is the volume of permeate collected between two weight measurements, A is the membrane surface area, and Δt is the time between two weight measurements. Salt rejection is calculated in the following Eq. (2):

$$R = \left(1 - \frac{C_p}{C_f}\right) \times 100\% \tag{2}$$

where R is the salt rejection parameter, C_p is the salt concentration in permeate, and C_f is the salt concentration in feed. The salt concentrations are measured using conductivity meter.

3. Results and discussion

3.1. Characterization of SWCNTs

The functionalized SWCNTs were characterized by TGA, HRTEM and XPS.

Fig. 1 shows the TGA thermograms of pristine SWCNTs and functionalized SWCNTs (A sample was heat-treated at a linear heating rate of 10°C/min up to 800ºC in a mixture of nitrogen and oxygen as protective gas). It shows that the sample decomposition temperature changed with different functional group. A slight weight loss around 180°C could be observed in five curves from Fig. 1, this weight loss was assigned to weight loss of moisture absorbed in the sample. The obvious weight loss of p-SWCNTs was at 410°C. After modification, the weight loss of SWCNT-COOH from 180°C to 426°C was assigned to the weight loss of COOH group and the loss rate was about 15%. For SWCNT-COCl, the weight loss rate was about 14% and the chloride was decomposed between 180°C and 460°C. Similarly, SWCNT-CONH$_2$ had a 13% weight loss, which attributed to the decomposition of amide. For SWCNT-NH$_2$, a 14% weight loss rate between 180°C and 410°C was assigned to the decomposition of amino group. These results can provide quantitative estimates of the degree of functionalization of SWCNTs.

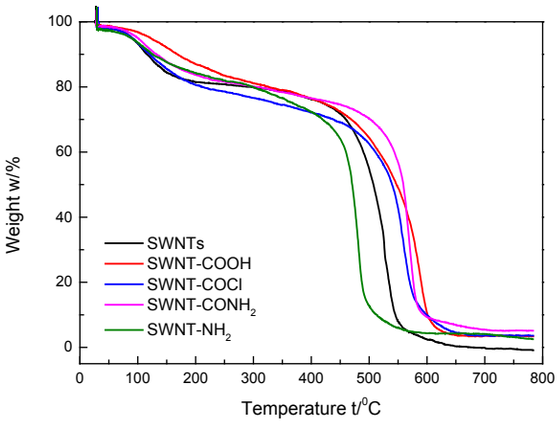

Fig. 1. TGA thermograms of SWCNTs, SWCNT-COOH, SWCNT-COCl, SWCNT-CONH$_2$, SWCNT-NH$_2$.

High resolution transmission electron microscopy (HRTEM) of pure and modified SWCNTs and the Gauss distribution curve of inner diameter of SWCNTs are shown in Fig. 2. It is clear that the pristine SWCNTs (a) were curled and agglomerated in aqueous solution, and almost all the tips of the pristine SWCNTs were closed. After functionalization, the samples were well dispersed in aqueous solution and showed a loose morphology. The tips of many SWCNTs were opened as shown in picture (b) (c) (d). In addition, the chemical treatment under the present condition did not cause any damage to the tubular shape. Moreover, the inner diameter distribution in Fig. 2 shows that the inner diameter of the pipe became narrower than the original one on the condition that the length of –COOH, –CONH$_2$ and –NH$_2$ were approximately 0.356 nm, 0.365 nm and 0.215 nm (the length data was obtained by molecular simulation, as shown in Fig. 2e), and the inner diameter difference between original SWCNTs and grafted SWCNTs was nearly equal to the length of corresponding functional group, which meant that the functional groups were successfully grafted interior to the SWCNTs.

Further, X-ray photo electron spectroscopy (XPS) was used to investigate whether carbon nano tubes grafted functional groups on the surface (see Fig. S1, S2, S3, S4 in the Supporting Information). Fig. S1 shows that the atomic concentrations of carbon (C 1s, 284 eV) and oxygen (O 1s, 531 eV) of P-SWCNT were 95.18% and 3.43%. Moreover, the sum of the carbon and oxygen was 1 if impurities were ignored. The binding energy of C element in P-SWCNTs could be deconvoluted into four peaks at 283.77, 284.81, 285.80 and 286.90 eV, which corresponded to C–C, C=C, C–H and C–O respectively. The O 1s spectra displayed two peaks at 531.7 eV and 533.39 eV, representing O–C and O–H. Fig. S2 shows that carboxylic was successfully attached to SWCNTs due to the significant increase of oxygen content (C 88.83%, O 14.77%). In addition, the peak fit of C and O element in Fig. S2b and S2c reconfirmed the successful attachment of COOH group on SWCNTs. A new elements chloride (Cl 2p, 198 eV) was also found in Fig. S3, proving that acyl chlorine was successfully

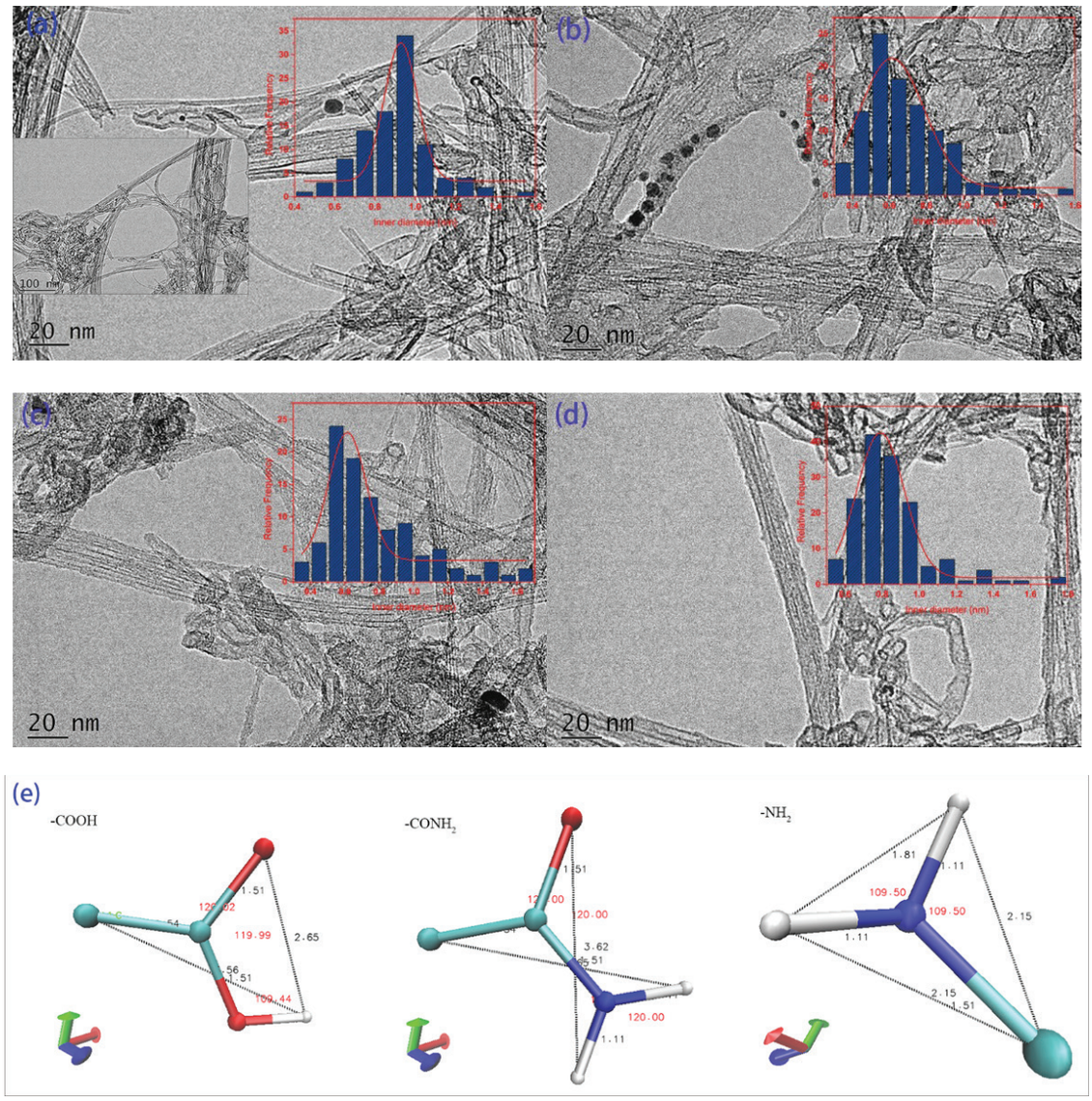

Fig. 2. HRTEM images of: (a) P-SWCNT, (b) SWCNT-COOH, (c) SWCNT-$CONH_2$, (d) SWCNT-NH_2. (e) The bond length of simulation.

grafted on SWCNTs with 0.75% content. The content of Cl 2p and O 1s was reduced to 0.31% and 7.57% respectively in Fig. S4. This implied that the amides have been generated. Comparing with the peak fit spectra of C and O in Fig. S4 and Fig. S5, the keys of C=O disappeared and turned into $–NH_2$, indicating that the carbonyl was replaced by amino. X-ray photo electron spectroscopy showed that the functional groups were grafted on the outer walls of SWCNTs.

3.2. Characterization of SWCNT-polyamide thin film nano composite membrane

The surface characteristics of membranes were studied by SEM images, salt rejection, water flux tests and surface contact angle analysis.

The SEM images of surface morphology of the polyamide and SWCNT-polyamide thin film nano composite membrane are shown in Fig. 3. Compared with the morphology of four composite membranes, the bare polyamide RO membrane had typical ridge and valley structures observed in PA membranes. Meanwhile, polyamide nano composite membrane containing SWCNTs had bigger nodules and showed more knot-like structures than polyamide membrane. That was because the embedded SWCNTs in the polyamide layer, or in other way, some globule-like structures were entangled to each other and formed a cross-linking area, making the roughness of the membrane surface reduced. There is high possibility that the decline of roughness of the SWCNTs embedded membrane attributed to the high hydrogen bonding between polyamide and the SWCNTs. When the surface SEM images of raw (B) and functionalized SWCNTs (C) (D) membranes were compared with each other, it was obvious that the surface morphologies were almost the same. This phenomenon may be

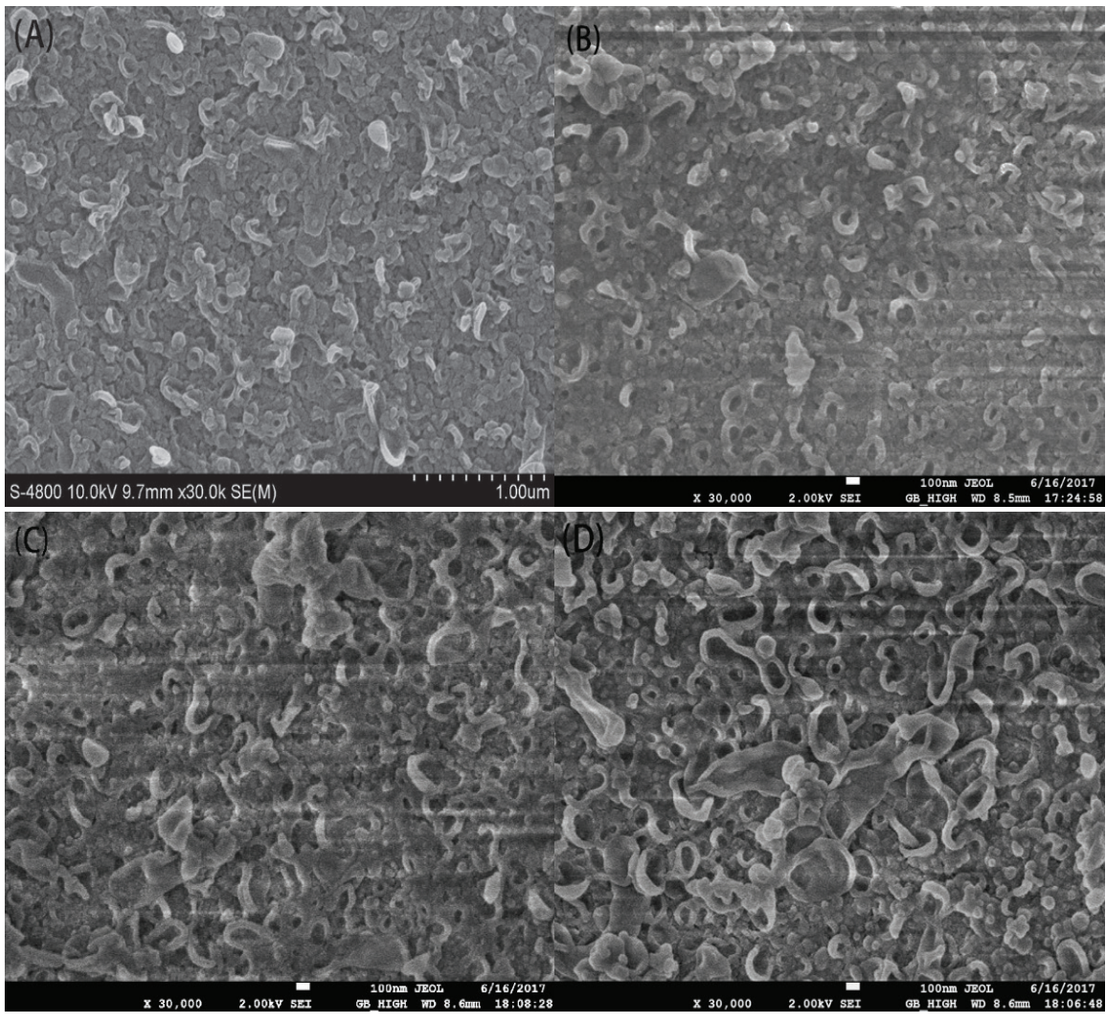

Fig.3. The SEM images of surface morphology of (A) PA, (B) PA-SWCNTs, (C) PA-SWCNT-COOH, (D) PA-SWCNT-NH_2.

related to the steady spread of single-walled carbon nano tube on surface of the membrane. It is worth mentioning that oxidized SWCNTs were definitely effective for increasing water flux and hydrophilicity thanks to the existing hydrogen bonds.

Water flux and desalination performance of the prepared various types of SWCNT-polyamide membrane (2000 ppm of NaCl feed solution, 2.0MPa of feed pressure) are given in Fig. 4. All membrane performance results shown in the figure were the average values obtained by more than three measurements from the three membrane samples prepared at different times. It is obvious from the figure that all of the SWCNT-polyamide membrane (especially the addition of hydrophilic groups such as carboxyl groups and amino groups, the desalination rate is as high as 99.214% and 99.357%, respectively) have higher salt rejection and water flux compared to the PA membrane. The increase of water flux resulted from the fact that the average inner diameter of both modified (0.6–0.7 nm) and unmodified (0.9 nm) SWCNT were highly bigger than PA

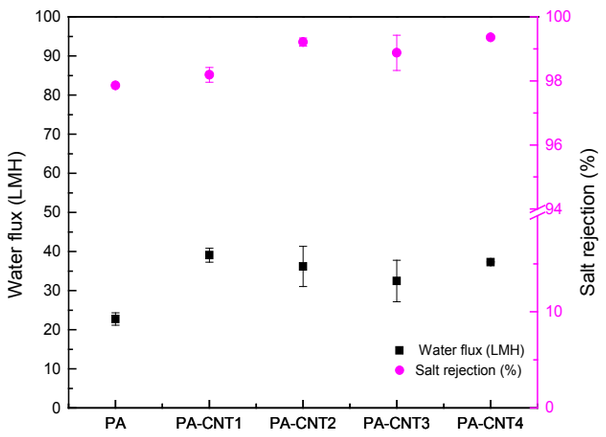

Fig. 4. Water flux and salt rejection of membranes prepared by various types of SWCNTs, (2000 ppm of NaCl feed solution, 2.0 MPa of feed pressure).

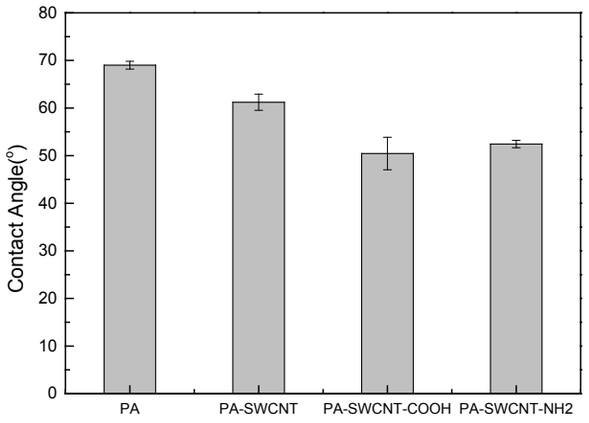

Fig. 5. Contact angle of the prepared poly amide membrane.

(0.1 nm), which allowed more water molecules to pass through. On the other hand, the addition of modified groups improved the carbon nano tubes hydrophilicity, which made water molecules easier to approach carbon nano tubes. For salt rejection, we have done a series of simulation, and the results showed that adding a certain number of functional groups to the inner wall could increase the rate of desalination greatly [24,25]. which resulted in the interaction between inner group (–COOH/–$CONH_2$/–NH_2) and ions: negatively charged group would attract positively charged Na^+ and held tightly (about 11.15kJ/mol) under 200 MPa pressure, at the same time, it could repelled Cl^- and prevent Cl^- from entering nano tubes due to electrostatic repulsions. The positively charged group was also the same principle.

The water contact angle of surface displayed its hydrophilic nature. Measured values of SWCNT-polyamide membrane water contact angle are plotted in Fig. 5, which shows that the contact angle exhibited a decreasing trend by adding SWCNTs, indicating that the hydrophilicity of PA-SWCNTs composite membrane was improved. The decease of contact angle was attributed to, on one hand, incorporating the functionalized SWCNTs with hydrophilic groups such as carboxyl groups and amino groups; on the other hand, the reduction of surface roughness.

4. Conclusion

Tip and inner walled carbon nano tubes were functionalized via an oxidative process using a mixture of concentrated sulfuric acid and nitric acid and then reacted by substitution reaction. The products were characterized by HRTEM, XPS, TGA and was confirmed that carboxyl, carbonyl chloride, amide and amine were successful grafted onto/into the SWCNTs. From the evaluation by membrane performance evaluation instrument, we could draw a conclusion that the water flux and salt rejection of SWCNT-polyamide membrane was increased obviously compared with bare PA membrane. In particular, the interior addition of hydrophilic groups such as carboxyl groups and amino groups, made the water flux and salt rejection of SWCNT-polyamide membranes improved dramatically.

Acknowledgments

This research was supported by the National Natural Science Foundation of China [No. 21306096].

References

[1] S. lijima, Helical micro tubules of graphitic carbon, Nature, 354 (1991) 56–58.
[2] B.R. Stoner, B. Brown, J.T. Glass, Selected topics on the synthesis, properties and applications of multi walled carbon nano tubes, Diam. Relat. Mater., 42 (2014) 49–57.
[3] A. Battigelli, C. Menard-Moyon, T. Da Ros, M. Prato, A. Bianco, Endowing carbon nano tubes with biological and biomedical properties by chemical modifications, Adv. Drug Deliver. Rev., 65 (2013) 1899–1920.
[4] M. Tarfaoui, K. Lafdi, A. El Moumen, Mechanical properties of carbon nano tubes based polymer composites, Composites, Part B, 103 (2016) 113–121.
[5] R. Di Giacomo, B. Maresca, M. Angelillo, G. Landi, A. Leone, M.C. Vaccaro, C. Boit, A. Porta, H.C. Neitzert, Bio-nano-composite materials constructed with Single cells and carbon nano tubes: mechanical, electrical, and optical properties, IEEE T NanoTechnol., 12 (2013) 1026–1030.
[6] R. Kotsilkova, E. Ivanov, E. Krusteva, C. Silvestre, S. Cimmino, D. Duraccio, Isotactic polypropylene composites reinforced with multi wall carbon nano tubes, part 2: Thermal and mechanical properties related to the structure, J. Appl. Polym. Sci., 115 (2010) 3576–3585.
[7] H.R. Darabi, M. Jafar Tehrani, K. Aghapoor, F. Mohsenzadeh, R. Malekfar, A new protocol for the carboxylic acid sidewall functionalization of single-walled carbon nano tubes, Appl. Surf. Sci., 258 (2012) 8953–8958.
[8] A. Gromov, S. Dittmer, J. Svensson, O.A. Nerushev, S.A. Perez-García, L. Licea-Jiménez, R. Rychwalski, E.E.B. Campbell, Covalent a mino-functionalisation of single-wall carbon nanotubes, J. Mater. Chem., 15 (2005) 3334.
[9] Y. Kanbur, Z. Küçükyavuz, Surface modification and characterization of multi-walled carbon nanotube, Fuller, Nanotub. Car. N., 19 (2011) 497–504.
[10] J. Kathi, K.Y. Rhee, Surface modification of multi-walled carbon nanotubes using 3-aminopropyltriethoxysilane, J. Mater. Sci., 43 (2007) 33–37.
[11] V.T. Le, C.L. Ngo, Q.T. Le, T.T. Ngo, D.N. Nguyen, M.T. Vu, Surface modification and functionalization of carbon nano tube with some organic compounds, Adv. Nat. Sci-Nano Sci., 4 (2013) 035017.
[12] C. Dong, A.S. Campell, R. Eldawud, G. Perhinschi, Y. Rojanasakul, C.Z. Dinu, Effects of acid treatment on structure, properties and biocompatibility of carbon nano tubes, Appl. Surf. Sci., 264 (2013) 261–268.
[13] Q. Wan, J. Tian, M. Liu, G. Zeng, Q. Huang, K. Wang, Q. Zhang, F. Deng, X. Zhang, Y. Wei, Surface modification of carbon nano tubes via combination of mussel inspired chemistry and chain transfer free radical polymerization, Appl. Surf. Sci., 346 (2015) 335–341.
[14] T. Kyotani, S. Nakazaki, W.-H. Xu, A. Tomita, Chemical modification of the inner walls of carbon nano tubes by HNO_3 oxidation, Carbon., 39 (2001) 782–785.
[15] Y. Hattori, Y. Watanabe, S. Kawasaki, F. Okino, B.K. Pradhan, T. Kyotani, A. Tomita, H. Touhara, Carbon-alloying of the rear surfaces of nano tubes by direct fluorination, Carbon, 37 (1999) 1033–1038.
[16] R. Sawicki, L. Mercier, Evaluation of mesoporous cyclodextrin-silica nano composites for the removal of pesti-

cides from aqueous media, Environ. Sci. Technol., 40 (2006) 1978–1983.
[17] J. Farahbakhsh, M. Delnavaz, V. Vatanpour, Investigation of raw and oxidized multi walled carbon nano tubes in fabrication of reverse osmosis poly amide membranes for improvement in desalination and anti fouling properties, Desalination, 410 (2017) 1–9.
[18] V. Vatanpour, M. Safarpour, A. Khataee, H. Zarrabi, M.E. Yekavalangi, M. Kavian, A thin film nano composite reverse osmosis membrane containing amine-functionalized carbon nano tubes, Sep. Purif. Technol., 184 (2017) 135–143.
[19] V. Vatanpour, M. Esmaeili, M.H.D.A. Farahani, Fouling reduction and retention increment of polyethersulfone nano filtration membranes embedded by a mine-functionalized multi-walled carbon nano tubes, J. Membr. Sci., 466 (2014) 70–81.
[20] A. Rahimpour, M. Jahanshahi, S. Khalili, A. Mollahosseini, A. Zirepour, B. Rajaeian, Novel functionalized carbon nano tubes for improving the surface properties and performance of polyethersulfone (PES) membrane, Desalination, 286 (2012) 99–107.
[21] L. Zhang, G.-Z. Shi, S. Qiu, L.-H. Cheng, H.-L. Chen, Preparation of high-flux thin film nano composite reverse osmosis membranes by incorporating functionalized multi-walled carbon nano tubes, Desal. Water Treat., 34 (2011) 19–24.
[22] H.J. Kim, Y. Baek, K. Choi, D.-G. Kim, H. Kang, Y.-S. Choi, J. Yoon, J.-C. Lee, The improvement of anti bio fouling properties of a reverse osmosis membrane by oxidized CNTs, RSC Adv., 4 (2014) 32802.
[23] H.J. Kim, K. Choi, Y. Baek, D.G. Kim, J. Shim, J. Yoon, J.C. Lee, High-performance reverse osmosis CNT/polyamide nano composite membrane by controlled inter facial interactions, ACS Appl. Mater Inter., 6 (2014) 2819–2829.
[24] Q. Li, D.F. Yang, J.S. Shi, X. Xu, S.H. Yan, Q.Z. Liu, Biomimetic modification of large diameter carbon nano tubes and the desalination behavior of its reverse osmosis membrane, Desalination, 379 (2016) 164–171.
[25] Q. Li, D.F. Yang, J.H. Wang, Q. Wu, Q.Z. Liu, Biomimetic modification and desalination behavior of (15,15) carbon nano tubes with a diameter larger than 2 nm, Acta Phys-Chim Sin., 32(X) (2016) 001–009.
[26] K.P. Lee, T.C. Arnot, D. Mattia, A review of reverse osmosis membrane materials for desalination—Development to date and future potential, J. Membr. Sci., 370 (2011) 1–22.
[27] H. Huang, X. Qu, H. Dong, L. Zhang, H. Chen, Role of NaA zeo lites in the inter facial polymerization process towards a polyamide nano composite reverse osmosis membrane, RSC Adv., 3 (2013) 8203–8207.

Supporting Information

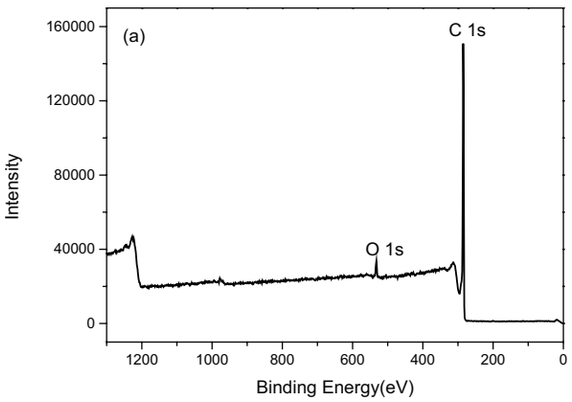

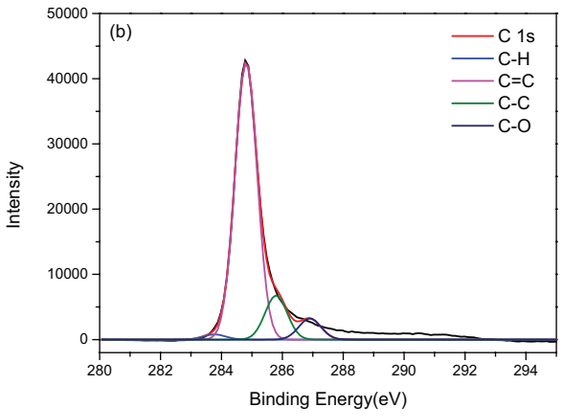

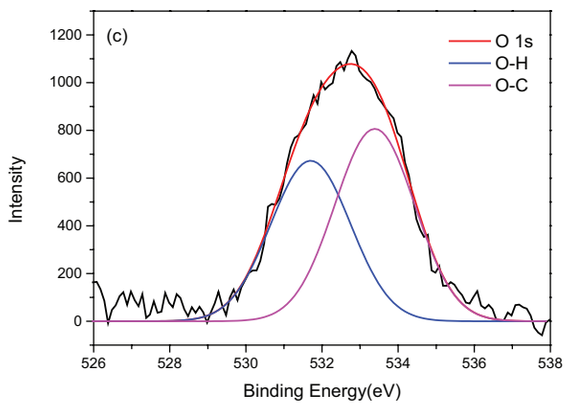

Fig. S1. (a) XPS spectrum of P-SWCNT, (b) C 1s, (c) O 1s.

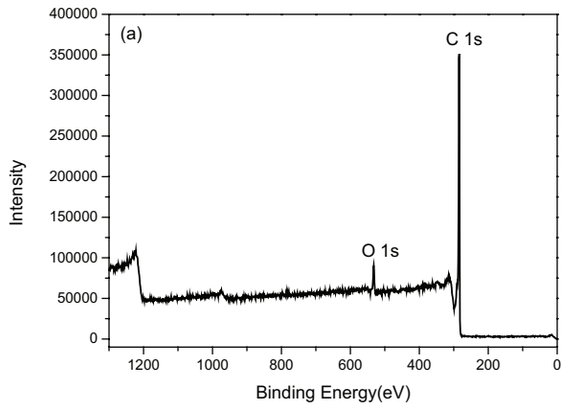

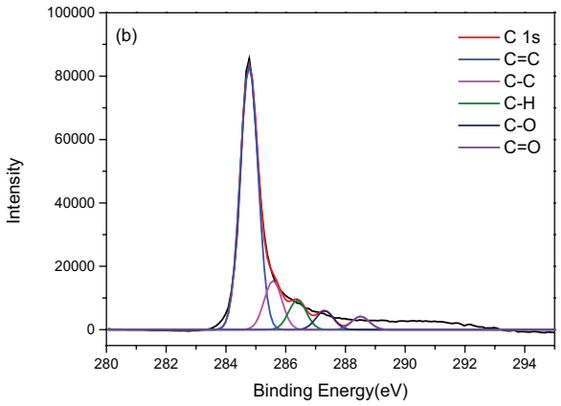

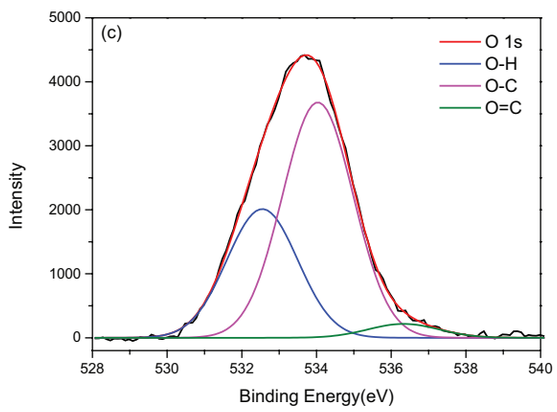

Fig. S2. (a) XPS spectrum of SWCNT-COOH, (b) C 1s, (c) O 1s.

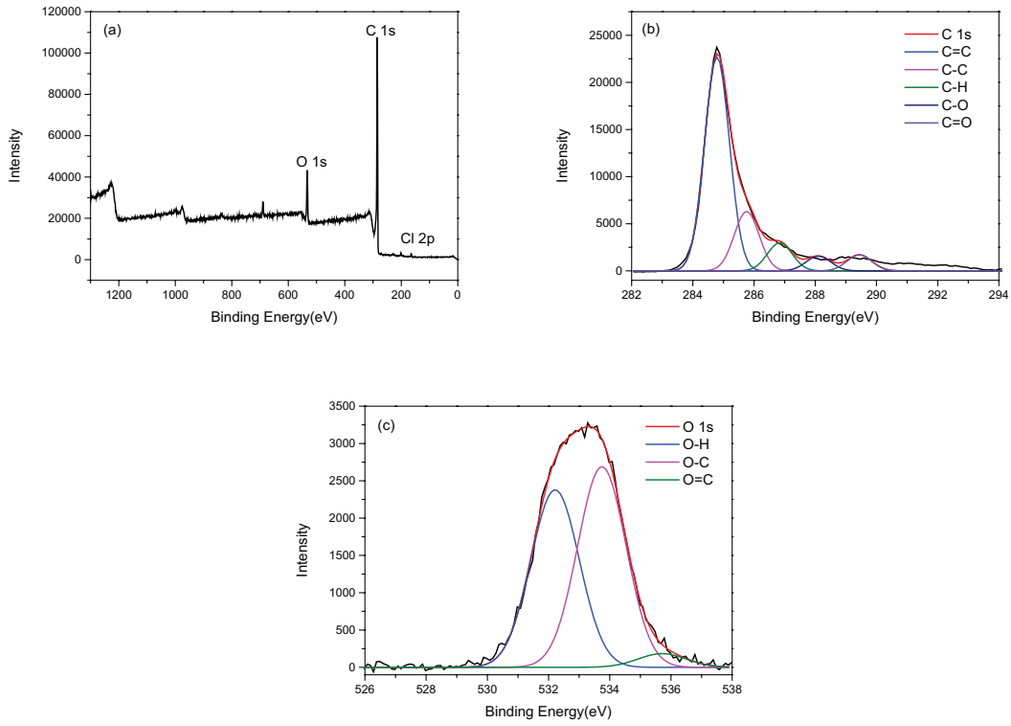

Fig. S3. (a) XPS spectrum of SWCNT-COCl, (b) C 1s, (c) O 1s.

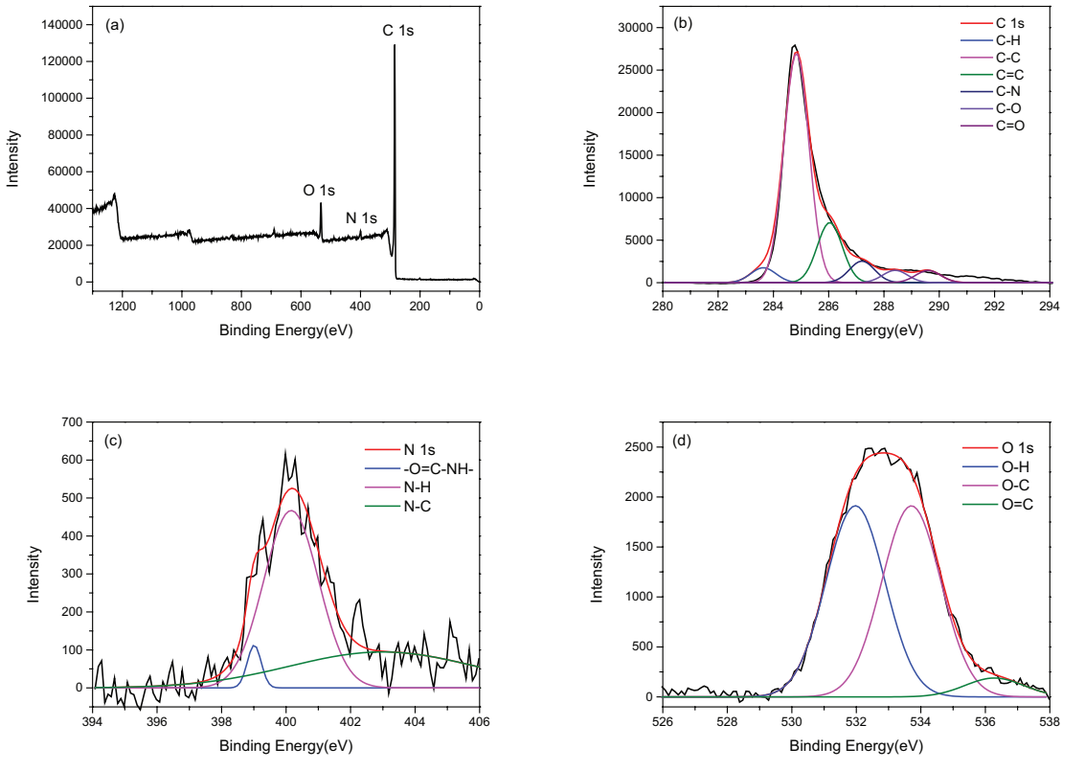

Fig. S4. (a) XPS spectrum of SWCNT-$CONH_2$, (b) C 1s, (c) N 1s, (d) O 1s.

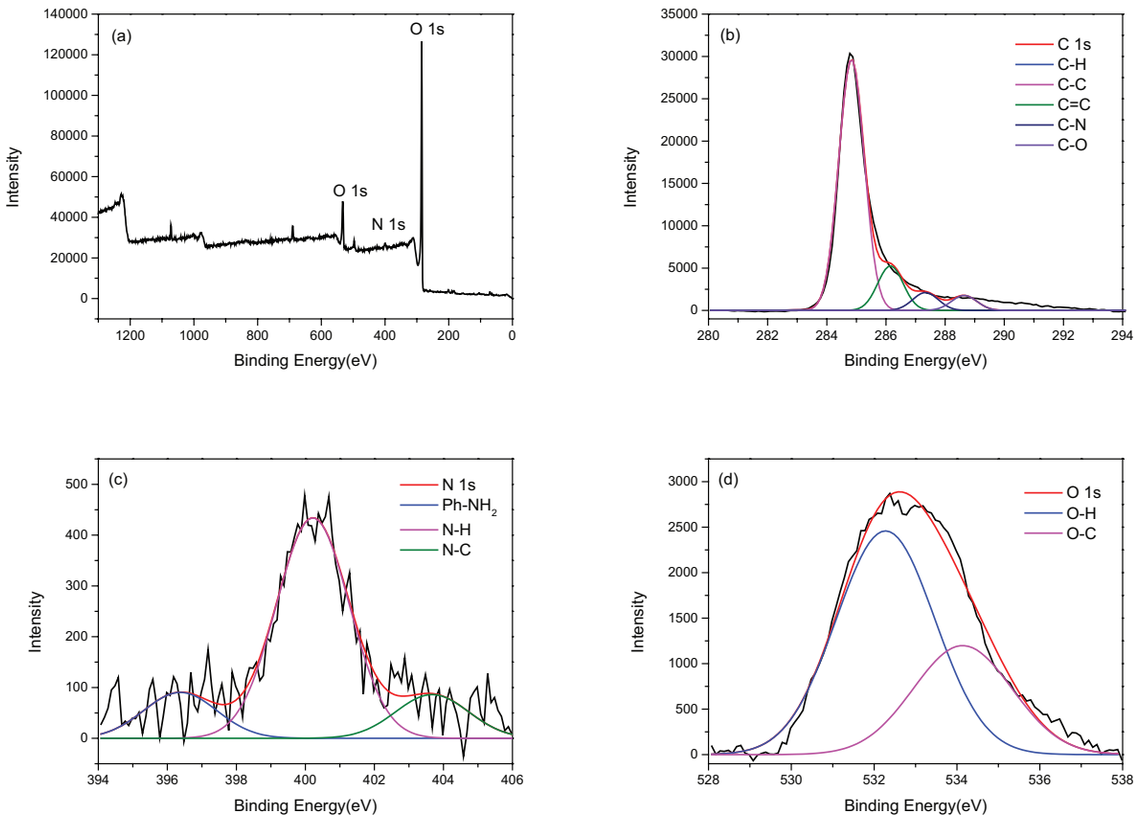

Fig. S5. (a) XPS spectrum of SWCNT-NH_2, (b) C 1s, (c) N 1s, (d) O 1s.